

# **Evidence for a Change to Aerosol Fractions: In a Gobi Town**

```
## -- Attaching core tidyverse packages ----- tidyverse 2.0.0 --
## v dplyr     1.1.4     v readr     2.1.5
## v forcats   1.0.0     v stringr   1.5.1
## v ggplot2   3.5.1     v tibble    3.2.1
## v lubridate  1.9.3     v tidyverse  1.3.1
## v purrr     1.0.2
## -- Conflicts ----- tidyverse_conflicts() --
## x dplyr::filter() masks stats::filter()
## x dplyr::lag()    masks stats::lag()
## i Use the conflicted package (<http://conflicted.r-lib.org/>) to force all conflicts to beco
```

Running title: INSERT RUNNING TITLE HERE

Munkhtsetseg. E, Shimizu. A, Matsuki. A, Batdorj. D, Matsui. H, Bayanjargal. D

To whom correspondence should be addressed:

1 Plain text summary Driven by industrial progress in the mining sector, household coal combustion  
2 has increased significantly in Mongolia since the 2000s. Demographic evidence has revealed an  
3 ongoing reduction in rural-nomadic lifestyle and a rise in urban population, which may gradually  
4 extend household winter heating as a major source of fine particulate matter (PM2.5). In  
5 conjunction with a stagnant atmosphere and observations that winter fine pollutants (PM2.5 and  
6 PM10) are persistently trapped within the boundary layer and can be exacerbated by stagnant  
7 weather or emission sources, these results have led to hypotheses that fine aerosols may be  
8 subject to suspension in the near-surface atmosphere, potentially available for emission via  
9 dust storms in the spring. Here, through the analysis of long-term datasets, we demonstrate  
10 distinct spatio-temporal patterns in variations of PM10 and PM2.5 relative to recent drivers of  
11 emission sources in Mongolia, and that the concentration of PM2.5 in a Gobi town has increased  
12 in association with winter heating. Furthermore, the ratio of fine to coarse aerosols indicates that  
13 the fine fraction in the spring has increased despite decreased wind speeds. Our results strongly  
14 suggest that the aerosol fraction has undergone changes at the local-level, and is subject to both  
15 natural and anthropogenic constraints.

16 **Abstract (150 words: 200, cut 50 words )**

17 Here, through the analysis of long-term datasets, we demonstrate distinct spatio-temporal patterns  
18 in variations of PM10 and PM2.5 relative to recent drivers of emission sources in Mongolia, and  
19 that the concentration of PM2.5 in a Gobi town has increased in association with winter heating.  
20 Furthermore, the ratio of fine to coarse aerosols indicates that the fine fraction in the spring  
21 has increased despite decreased wind speeds. Our results strongly suggest that the aerosol  
22 fraction has undergone changes at the local-level, and is subject to both natural and anthropogenic  
23 constraints.

24 **Introduction /Why you should care/**

25 Gobi Desert is known for its high dust storm frequency and substantial dust emissions, precise  
26 quantification of its contribution to the global dust budget is somewhat simplified. It is well defined  
27 that Mongolian dust has a brown color, seasonal characteristics, mainly consisted coarse fractions.  
28 Mongolian dust has an attention of the its mass fraction in global dust, yet unlikely elaborated in  
29 the climate models due to its majority of coarse fraction for its a small contribution to the climate  
30 system through its radiative feedback. But, such recognized characterization might get no longer  
31 valid due to recent change in the driving of the emissions of air particulate matters. POINT 1:  
32 AEROSOL EFFECTS ON radiation POINT 2: COLD DESERTS, POINT 3: AIR QUALITY AND  
33 HEALTH

34 Aerosols from cold arid areas, particularly the Gobi Desert in Asia, constitute the second most  
35 substantial global source of atmospheric aerosols (Fitzgerald et al., 2015). These dust particles  
36 considerably impact Earth's radiative equilibrium by directly scattering solar radiation and serving  
37 as nuclei for cloud droplet and ice crystal formation, while also influencing climate through its  
38 interactions with solar radiation (Huang et al. 2014), clouds (Kawai et al. 2021), and terrestrial and  
39 oceanic biogeochemistry (Jickells et al. 2005; Mahowald et al. 2017). This dust is carried towards  
40 the North Pacific by prevailing westerly winds (Husar et al. 2001; Uno et al. 2009), significantly  
41 affects local and regional air quality (Sugimoto et al. 2003; Jugder et al. 2011) and human health  
42 (Higashi et al. 2014).

43 There has been a [tremendous improvement] in the understanding of atmospheric aerosols  
44 and their climate effect over the last decades, with some important observational and modelling  
45 breakthroughs. Long-term measurements of aerosols (e.g., Nishikawa et al. 2010, Andrews et  
46 al. 2011), observational campaigns (e.g., Shinoda, Park, chinse), and lidar (Holben et al. 1998,  
47 Remer et al. 2008), and bioaerosol (dd), health (ff) have remarkably increased knowledge  
48 about the composition and characteristics of atmospheric aerosols. dust brown color, seasonal  
49 characteristics, with coarse fractions. Gobi Desert dust typically has a shorter atmospheric  
50 residence time (1.5 days) tends to remain at lower altitudes, (Tanaka, 2012) During dust storms,  
51 PM<sub>2.5</sub> and PM<sub>10</sub> concentrations can surge to 343 and 1.642  $gm^3$ , respectively (Filonchyk et al.,

52 2021). Regarding aerosol fractions, PM2.5 and PM10 concentrations in the Gobi Desert area  
53 were found to be  $36.2 \pm 23.7$  and  $97.3 \pm 84.5 \text{ gm}^3$ , respectively (Filonchyk et al., 2021). Clean  
54 continental aerosol type is predominant (73.9 percent), followed by mixed aerosols (20.4 percent),  
55 with minor contributions from clean marine, urban/industrial, biomass burning, and desert dust  
56 aerosol types. During dust storms, PM2.5 and PM10 concentrations can surge to 343 and  $1.642 \text{ gm}^3$ ,  
57 respectively (Filonchyk et al., 2021) Gobi Desert is known for its high dust storm frequency  
58 and substantial dust emissions, precise quantification of its contribution to the global dust budget  
59 is challenging. Nevertheless, the land surface parameters governing Asian dust emissions exhibit  
60 substantial seasonal and inter-annual variations and complex interactions, leading to significant  
61 uncertainties in simulating them for Asian dust (Kawai Sola 2021).

62 Advanced the knowledge of global dust, has reached to recognize the sources,. Classification  
63 dust brown color, seasonal characteristics, with coarse fractions. Much studies, The Gobi Desert  
64 is a primary source of global atmospheric aerosols, with dust emissions heavily influenced by wind  
65 strength and surface dust availability (Liang et al., 2021). Gobi Desert dust typically has a shorter  
66 atmospheric lifetime (1.5 days) compared to Taklimakan Desert dust (2.1 days) (Tanaka, 2012),  
67 indicating differences in transport patterns and atmospheric persistence (Tanaka, 2012). Gobi dust  
68 tends to remain at lower altitudes, while Taklimakan dust can be transported to higher elevations,  
69 potentially contributing to the Asian tropopause aerosol layer (Tanaka, 2012). Gobi Desert is  
70 known for its high dust storm frequency and substantial dust emissions, precise quantification of  
71 its contribution to the global dust budget is somewhat simplified. It is well defined that Mongolian  
72 dust has a brown color, seasonal characteristics, mainly consisted coarse fractions.

73 This knowledge further efficient to climate system when elaborating dust-aerosol effects. But,  
74 a large uncertainties in the global dust model has existed so for climate models which clearly  
75 limits our understanding the climate system and shape the facing global issues of global warming.  
76 This is first mainly, caused by the lack of parameterization and the complex nature of its aerosol  
77 composition. [AND] surface ... [AND] anthropogenic, livestock These findings highlight the  
78 significant contribution of the Gobi Desert to global dust aerosols and the complex nature of its  
79 aerosol composition.

80 Second, the significant contribution of the Gobi Desert to global dust aerosols is not fully  
81 recognized; and their is the rapid growing changes controlled by the natural forces and  
82 anthropogenic drivings. Mongolian dust has an attention of the its mass fraction in global dust,  
83 yet unlikely elaborated in the climate models due to its majority of coarse fraction for its a small  
84 contribution to the climate system through its radiative feedback. ... Rapid change ; few research;  
85 needs to enroll such changes and multidisciplinary

86 But, such recognized characterization might get no longer valid due to recent change in the driving  
87 of the emissions of air particulate matters. A large high concentrations of PM2.5 in the capital  
88 city of Mongolia has been observed as a result of the heavy consumptions of coal as a winter  
89 heating has rapidly spread as a mining industry taken off since 2000. Demographic evidence has  
90 revealed an ongoing reduction in rural-nomadic lifestyle and a rise in urban population, which may  
91 gradually extend household winter heating as a major source of fine particulate matter (PM2.5).  
92 Winter weather stagnant conditions governed by the Siberian magnifies the concentrations of the  
93 particulate matter emissions by trapping the polluted air below the boundary layer, so that results  
94 in a very large high concentrations of PM2.5, locally. Even within a short span, UB has recognized  
95 as one of the highly polluted capital cities in the world.; resulted a human health issues.

96 Therefore, It is important to examine the emerging changes and shifting patterns of air particulate  
97 matters in Mongolia. More importantly, it is essential to reveal the significant changes in the the  
98 altered fraction particularly, in the dust seasons considering its high potential of intriguing in the  
99 free atmosphere to transported in the long-distance, so carrying capacity of the role to shift the  
100 global climate system, and its side impacts on downwind regions.

- 101 • Study goal - We hypothesize ... - Our study will benefit not only to the global dust research  
102 but also climate, and further to the country itself for urban planning, and coal combustion.

103 **Research Qs**

104 Therefore, we aimed to demonstrate the distinct temporal and spatial variations of PM2.5 and  
105 PM10 across urban and rural Mongolia using extensive data from 2008 to 2020.

106 On spring, the dust storm from the Gobi Desert contribute significantly to increased aerosols in the  
107 atmosphere and ambient air pollution, leading to sporadic peaks in PM10 concentrations reaching  
108 as high as  $64\text{-}234 \text{ gm}^3$  per day or exceeding  $6000 \text{ gm}^3$  per hour (Jugder). concentrations of  
109 particulate matter is ephemeral, yet vary depending on whether the pollution cause is natural or  
110 industrial, local or transported, seasonal or non-seasonal, makes complex and challenging.

111 1. Do concentrations of particulate matters differ in between urban and rural sites, and even  
112 within Gobi sites? 2. Do distinct temporal variations has existed among the sites? 3. Do  
113 PM2.5 particulates has contributed to the PM10 annual variations?

114 • If yes, how much, and when and where?

115 • What is the sd, mean, and median

116 – box plot

117 – violin

118 – scatter points, epidemic, sporadic

119 • Daily variations to examine it related to the heating

120 – 2 peaks: smaller and bigger

121 – compare the t-duration exceeds  $50 \text{ mug/m}^3/\text{hour}$

122 4. Does it has distinct patterns among the sites regarding to the drivings

123 • How PMs varies with the wind speed and visibility

124 • Do they differently explained with variables and changes in drivings (with PCA analysis)

125 5. Is there any significant changes in time-series of PMs at 4 seasons

126 6. Is there any significant changes in ratio in the spring in respect to winter pollutions?

127 **Results**

128 **The spatio-temporal variations of the PMs at the study sites**

129 To evaluate the spatial variations in particulate matter (PM) concentrations, we displayed hourly  
130 observed values of PM10 and PM2.5 for all study sites (figure\_3). The mean p-values indicate  
131 that PM concentrations differ significantly at a 99% confidence level across all sites (figure\_3),  
132 with the exception of a 95% confidence level between DZ and UB for PM10 (figure\_3a),  
133 highlighting substantial concentration disparities among sites. While quantitative differences  
134 in PM concentration values exist across all sites, two key patterns emerge when examining  
135 median deviations from mean values and irregular observation fluctuations. For instance, PM10  
136 demonstrates more erratic behavior than PM2.5 at each location, particularly evident at ZU and  
137 SS sites. Furthermore, the mean values calculated from hourly measurements surpass the  
138 median concentrations for both PM10 and PM2.5 across all sites, with notable prominence at UB  
139 and DZ locations. Consequently, significant spatial differences in PM concentrations exist among  
140 all sites, regardless of urban or rural classification. However, the sites can be categorized into two  
141 groups based on their characteristics: UB (urban) and DZ (rural town, Gobi); and SS (rural, Gobi)  
142 and ZU (rural, Gobi). These findings for DZ appear to support our hypothesis of emerging new  
143 emission patterns related to increased coal consumption during winter months.

144 To investigate whether emerging PM patterns are associated with household winter heating  
145 activities, we demonstrated annual variations in PM10 and PM2.5 concentrations at the sites.

146 Significant annual variations in PM10 and PM2.5 levels were observed at UB and DZ sites,  
147 with maximum concentrations exceeding  $100 \text{ g/m}^3$  during colder months (January, November,  
148 December) and lower levels consistently below  $50 \text{ g/m}^3$  during warmer months (May-September).

149 These annual maximums coincided with the diurnal variations in PM10 and PM2.5 concentrations  
150 at sites DZ and UB, where PM concentrations reached their highest values during nighttime and  
151 early morning hours (approximately 8 PM to 4 AM UTC), with median values surpassing  $50 \text{ g/m}^3$ .  
152 Conversely, both pollutants exhibited reduced concentrations during daytime hours (8AM to 4PM  
153 UTC), likely due to increased atmospheric dispersion. UB site exhibited similar daily fluctuations  
154 with extended periods (approximately 8 PM to 5 AM UTC) of elevated concentrations. Additionally,  
155 winter PM10 concentrations at both sites were primarily composed of PM2.5 (figure\_5; mean  
156 values for PM10 with the color bar). The increase in PM10 and PM2.5 aligns with the heating  
157 active hours, suggesting that household coal consumption contributes to elevated PM levels at  
158 both DZ and UB sites. In contrast, ZU and SS sites displayed significantly lower annual PM10 and  
159 PM2.5 levels, with sudden frequent spikes in spring followed by occasional instances in autumn.  
160 These annual variations were more pronounced in PM10 compared to PM2.5, highlighting the  
161 impact of Gobi dust and sand storms. Similar occurrences were also noted at the DZ site,  
162 suggesting its exposure to both winter heating emissions and natural spring dust, reflecting its  
163 Gobi-region characteristics. The annual variability in PMs with higher concentrations during  
164 nighttime and colder months, indicating the influence of localized emission sources and reduced  
165 boundary layer mixing at UB and DZ sites. Additionally, the upward extended ranges without  
166 the bottom bottle of the violin plot, demonstrating greater variability during colder months. It  
167 implies instability in concentrations potentially reaching high levels above  $400 \text{ g/m}^3$  when Arctic  
168 oscillation/Siberian high intensifies with heating, and dropping below  $50 \text{ g/m}^3$  when it weakens or  
169 heating demand decreases. These findings confirm the (DZ) emerging PM pattern is caused by  
170 household activities and influenced by meteorological conditions. Overall, meteorological factors  
171 appear to play a crucial role in governing PM levels.

## 172 **The emission patterns of interrelations among meteorological variables at the study sites**

173 add table, add r 1.3, 2 on figure\_6, add supplement figures

174 To identify the key factors influencing PM emissions, we examined the relationships between wind  
175 speed (WS), visibility (VIS), and particulate matter (PM10 and PM2.5) concentrations across the

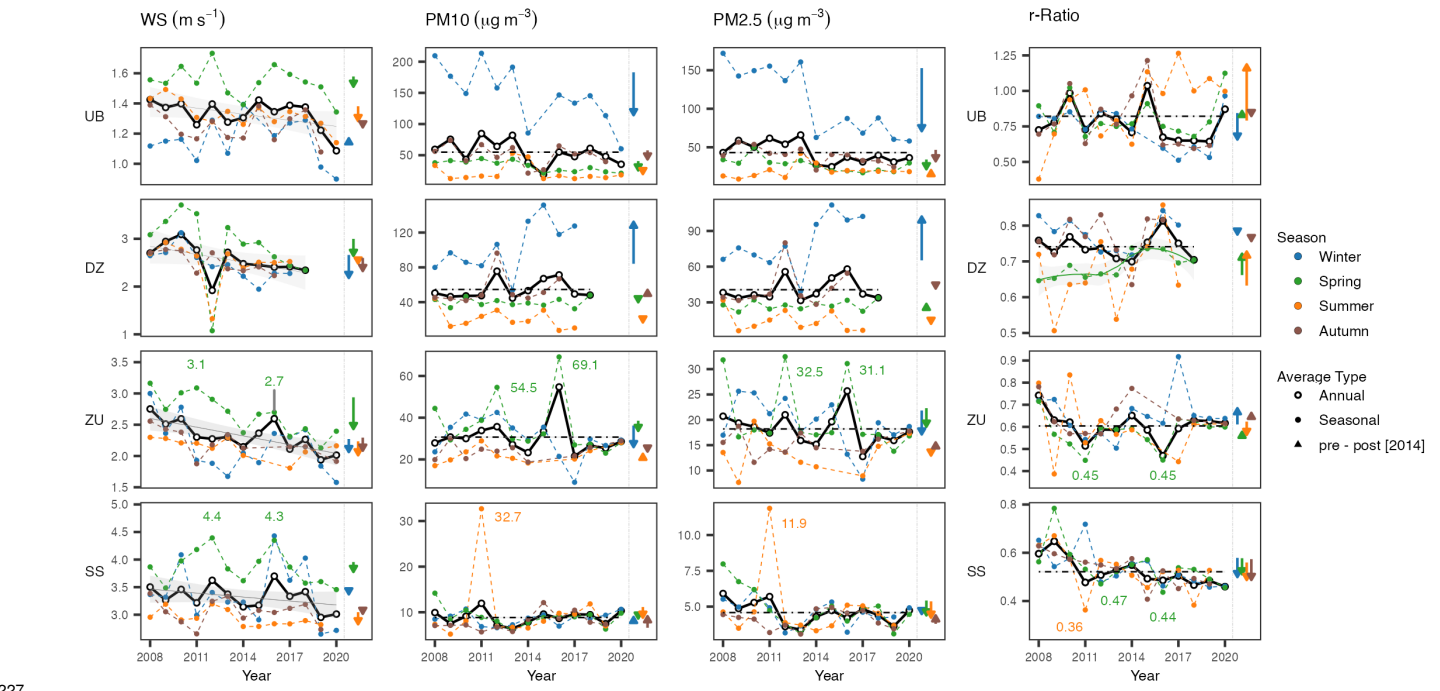
study sites (figure\_6). In UB during winter, elevated PM levels typically coincide with low wind speeds and reduced visibility (indicated by darker blue points). Notably, at DZ and ZU locations, high PM<sub>10</sub> concentrations were observed during both low and high wind speed conditions in winter. All Gobi sites exhibit the greatest variation in PM concentrations during spring, with extreme outliers primarily associated with increased WS and reduced visibility below 10000 km. Similar findings were also revealed through Principal Component Analysis (PCA). The initial two principal components (Dim 1 and Dim 2) account for 66.52% of the total variance. Dim 1 shows a strong association with PM<sub>10</sub> and PM<sub>2.5</sub>, while visibility demonstrates an inverse correlation, suggesting that reduced visibility corresponds to higher pollution levels. Wind speed and direction align positively with Dim 2 (22.16%), reflecting their impact on emissions. When comparing PM<sub>10</sub> aligns with PM<sub>2.5</sub>, the 1:1 ratio increases approximately 1.3 times for UB, 2 times for DZ, XXX for ZU, and XXX for SS as PM<sub>10</sub> concentrations increase. This increase in Gobi sites further escalated up to 2-5 times in ZU, and XXX times in SS sites, indicating insufficient PM<sub>2.5</sub> particulates in those locations, particularly at the ZU site. It is worth noting that instances where PM<sub>2.5</sub> values exceed PM<sub>10</sub> reflect equipment accuracy, correction errors, and higher sensitivity rates (ability to record emissions such as smoking near the sensor area). However, this discrepancy diminishes as PM concentrations increase, validating that higher observational records of PM<sub>2.5</sub> compared to PM<sub>10</sub> do not invalidate our results. Furthermore, clustering of monitoring sites based on PM concentrations and geographic features (Figure 7b) reveals distinct patterns. UB (urban, capital city) is characterized by high PM concentrations (positive Dim 1 scores), while SS (rural, Gobi, town (site located in the prevailing wind above the town)) shows low PM levels, clustering tightly along the negative Dim 1 axis. DZ (rural, Gobi, town center) displays considerable variability, with clusters extending into higher Dim 1 and Dim 2 ranges, reflecting the complex interplay of emission sources and meteorological factors. ZU (rural, Gobi, village) overlaps with SS but exhibits greater spread, indicating moderate pollution levels influenced by seasonal and localized factors. These findings highlight the complex interplay of spatial, meteorological, and local factors influencing air particulate matter concentrations across the studied locations and emphasizing the need for considering not only regional influences but also site-specific characteristics.

fig caption: the Principal Component Analysis (PCA) bi-plot (Figure 7a) highlights the relationships

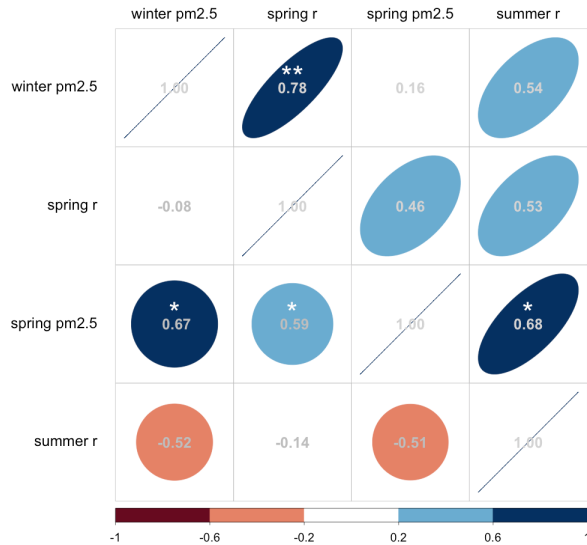
205 among key variables, including PM10, PM2.5, wind speed (WS), wind direction (WD), visibility,  
206 ratio of PM2.5 to PM10 (r), and numbers of aerosols by optical particle counter (OPC). The first  
207 two principal components (Dim 1 and Dim 2) explain 66.52% of the total variance, with Dim 1  
208 (44.36%) strongly associated with PM10 and PM2.5. Wind speed and wind direction are positively  
209 aligned with Dim 2 (22.16%), reflecting their influence on pollutant dispersion.

210 **The trends in concentrations of PMS and fine-coarse fractional changes at the sites**

211 **Seasonal and annual trends** Figure 8 illustrates the trend analysis of PM10 and PM2.5  
212 concentrations across study sites from 2009 to 2020. The time series demonstrates seasonal  
213 patterns and trends, with p-values of trend changes, seasonally: winter (Q1), spring (Q2), and  
214 summer-autumn (Q3). At UB, significant negative trends both in PM10 and PM2.5 concentrations  
215 are observed for winter and spring (Q1 and Q2,  $p < 0.001$ ). At DZ, a significant positive trend  
216 in PM10 and PM2.5 concentrations is observed for winter (Q1,  $p < 0.001$ ), indicating increasing  
217 particulate matter levels during this season. At ZU, a significant negative trend is observed in  
218 both PM10 and PM2.5 for winter (Q1,  $p < 0.001$ ), suggesting a consistent reduction in particulate  
219 matter during winter months (may reduced transboundary traffic associated with covid periods,  
220 resulted in declined PM10 concentrations; or data gaps). At SS, a negative trend is observed  
221 in PM2.5 for spring (Q2,  $p < 0.001$ ), reflecting a seasonal decline potentially linked to reduced  
222 wind speed during spring. The significant decreasing trends in PM concentrations in UB during  
223 colder months likely indicate improvements in emission control measures and a transition to more  
224 efficient heating practices. In contrast, a significant increasing trend is observed at DZ, particularly  
225 during winter (Q1), suggesting rising emissions potentially associated with urbanized household  
226 practices and other local activities in Mongolia's regional towns.



227



228

229 **r-ratio in spring when dust** Dust particles are emitted from the surface to the atmosphere when wind speed on the surface (i.e., friction velocity)  $u^*$  exceeds a threshold value  $u^{*t}$ , which is determined from soil particle size and land surface conditions (Shao 2008). In the case of Asian dust,  $u^{*t}$  is controlled by a number of land surface parameters such as snow cover, soil moisture, soil crust, soil freezing, and vegetation (Kurosaki et al. 2011), reflecting the location of

234 its source regions (mainly the Gobi and Taklimakan Deserts) at middle latitudes and high altitudes.

235 **Conclusions**

236 Arctic oscillation, the atmospheric system most influenced by global warming, triggers Arctic-Asian  
237 Dust with its potential phase changes (). Understanding how Arctic oscillation may interact with  
238 variability of concentrations in particulate matter (PM) in colder regions will contribute to the  
239 comprehension of these climate-teleconnection systems and their anthropogenic feedback  
240 mechanisms. Assessments of how aerosol fractions in the Gobi dust source region are affected  
241 by anthropogenic factors will provide better predictions of dust-aerosols and facilitate the reduction  
242 of household emissions under future climate scenarios. This information becomes increasingly  
243 significant if the negative phase of arctic oscillation intensifies and subsequent cold intensity and  
244 frequency increase with global climate change, as some models predict (....). In addition to  
245 changes in aerosol fraction, a warming climate will be driven by it as a key factor influencing the  
246 Earth's radiative energy balance.

247 In general, aerosols increase the outgoing solar radiation at the top of the atmosphere (TOA)  
248 through reflection, thus producing a planetary cooling effect. However, aerosols can also produce  
249 a warming effect due to increased reflected radiation from the surface, which enhances the  
250 aerosols' absorption. Recent shifts in surface types and their corresponding fine particulates,  
251 driven by both human activities and natural processes, raise a pivotal and yet unresolved question:  
252 How do these alterations impact the radiation budget of the Earth?

253 This research provides crucial insights into the complex interplay between Arctic oscillation,  
254 aerosol fractions, and climate change in Mongolia's Gobi Desert region. By analyzing long-term  
255 datasets of PM10 and PM2.5 concentrations, we have uncovered distinct spatio-temporal patterns  
256 and trends in aerosol fractions, revealing the significant impact of both natural processes and  
257 human activities on air quality and climate dynamics.

258 Our findings demonstrate that the fine-to-coarse aerosol ratio has increased in the Gobi region,  
259 particularly during spring, suggesting a shift in aerosol composition towards finer particles. This

260 change is likely driven by anthropogenic activities, especially winter heating, which contributes to  
261 the accumulation of fine pollutants in the atmosphere. The persistence of these pollutants through  
262 spring, combined with natural dust emissions, indicates a fundamental alteration in the aerosol  
263 profile of Mongolian Gobi dust.

264 These changes in aerosol composition have significant implications for regional and global  
265 climate systems. While aerosols have traditionally been associated with planetary cooling through  
266 increased reflection of solar radiation, our research highlights the growing importance of fine  
267 aerosol fractions in contributing to warming effects. This shift challenges existing assumptions  
268 about aerosol-climate interactions and underscores the need for more nuanced climate models  
269 that account for these complex dynamics.

270 The study also emphasizes the critical role of human activities in shaping regional air quality  
271 and climate patterns. The observed increase in PM2.5 concentrations in Gobi towns, particularly  
272 associated with winter heating, illustrates the tangible impact of anthropogenic emissions on  
273 local environments. This finding underscores the importance of targeted interventions to reduce  
274 household emissions, especially during winter months, as a means of mitigating both local air  
275 quality issues and broader climate impacts.

276 Our research opens up several avenues for future investigation, including the study of winter  
277 pollutant behavior during spring thawing, the transformation of black carbon during deposition  
278 and transportation, and the broader environmental implications of changing aerosol fractions.  
279 Additionally, the potential consequences of continued coal use and population growth on PM2.5  
280 levels and global climate systems warrant further examination.

281 In conclusion, this study contributes significantly to our understanding of the complex relationships  
282 between aerosols, atmospheric systems, and climate dynamics in the Gobi Desert region. By  
283 bridging critical knowledge gaps and providing evidence of changing aerosol compositions and  
284 their impacts, our findings offer valuable insights for refining climate models, informing policy  
285 decisions, and developing strategies to mitigate the effects of climate change. As we continue  
286 to grapple with the challenges of a changing climate, research such as this will be instrumental in  
287 guiding our efforts to create a more sustainable and resilient future.

288 The present study will contribute significantly to the understanding of air particulate matter  
289 patterns in Mongolia and providing comprehensive data insights for policymakers and public  
290 health sectors. Our findings is useful not only for addressing national health impacts but  
291 also beneficial for understanding air particulate matter as ambient air pollution, and tackling  
292 atmospheric aerosol effects in the climate system, and revealing their transboundary effects to  
293 the downwind regions in South-east Asia.

294 2. Summarize the main findings Novel conclusions: that change/advance our understanding of  
295 the field

296 3. Interpret the results within a broader context

297 In this study, Spatio-temporal distinct patterns in variations of  $PM_{10}$  and  $PM_{2.5}$  relative to the  
298 recent drivings of emission sources in Mongolia we investigated the temporal variations of PM2.5  
299 and PM10 concentrations at the 4 sites of rural and urban those located along the the wind corridor.

300 Air particulate matter concentrations in urban-town sites of UB and DZ is episodically dictated  
301 by dust events in spring or late autumn, yet seasonally governed by anthropogenic emissions in  
302 winter. Air particulate matter concentrations in rural sites of SS and ZU is episodically dictated  
303 by dust events in spring or late autumn. Air quality in urban sites is episodically dictated by dust  
304 events in spring or late autumn, yet seasonally governed by anthropogenic emissions in winter.  
305 [Air quality is governed by natural dust emission, and anthropogenic emissions]

306 Three distinct variations has been detected. 1. A new pattern is emerged It is evident of the new  
307 emission patterns in Mongolia. With recent growing interest in urban life style, and combustion of  
308 coal/oyutolgoi for heating winter conditions results a highly increase in not only capital city but also  
309 towns

310 In a result, spring coarse dust, plus winter fine pollutants Related to the winter emission patterns,  
311 fine particulates fraction in the spring is increased. r ratio shows ... emission source; dust  
312 might carry anthropogenic fine particulates as well. [spring coarse dust is immediately transported  
313 and deposited in the source area, whereas winter fine pollutants is permanently stayed in the  
314 source area due to stagnant atmosphere govern over entire country., perhaps floating in the near

315 surface, deposits in the surface] We found spring fine to coarse fraction has increased in a Gobi  
316 town, suggesting winter fine pollutants is permanently stayed in the source area due to stagnant  
317 atmosphere might related to AO, is emitted in the spring with the dust. This indicates the Mongolian  
318 Gobi dust aerosol fractions has changed with a more fine pollutants, so has an aerosol radiation  
319 effects.

320 • Alarms, the Mongolian dust in the spring, optical properties will be shifted; this gives . . . Gobi  
321 dust and sand storms has become tuiрен, from the shoroон шуурга. which clearly requires  
322 the attention. Main conclusion 1: A distinct pattern is emerged as a . . . Main conclusion 2:  
323 Trends in atmospheric fine particulate concentrations since 2008 were driven and modified  
324 by anthropogenic emissions in DZ Main conclusion 3: Trends in fine to coarse fraction is  
325 increased in the spring in DZ Main conclusion 4: WS is decreased; with the wind speed up  
326 to. . . Main conclusion 5: Such changes is local. Main conclusion 6: Our study highlighted  
327 the attribute of Gobi dust as a cold desert, with the anthropogenic impact.

328 4. Point limitations/alternate interpretations

329 5. Describe implications for other systems

330 6. List practical applications National level; meteorological impact is large. . . However,  
331 reduced. . . On the other hand, it is . . . with the towns. This points that air quality will  
332 be poor whether it is changed fuel, . . unless to change heating system. Therefore, it is not  
333 the reason to move the capital city. Only solution is to change the heating system, do not  
334 burn any type of the coal.

335 7. Suggest areas for future research

336 • Winter pollutants state in the land surface go under chemical reaction as soil thawing process  
337 in the spring or invoke the airborne infection?  
338 • black carbon, has a death records. In winter, it has detrimental effects on local; in spring, it  
339 will bring the effect on the downwind regions. More dangerously, how much it changed its  
340 initial form during the depositions and transportation period. More, research has focused on

341 the direct emission of black carbon to the atmosphere. However, it is not clear the changed  
342 form of black carbon on its properties, and chemical compositions so on.

- 343 • Other environmental problems?
- 344 • If continued use of coal, with the population increase result the more and more pm2.5, and  
345 affect Climate system.

346 The findings not only contribute to our understanding of the climate impacts of aerosol and surface  
347 albedo, but also emphasize the importance of integrating these factors into climate models and  
348 strategies aimed at mitigating climate change.

349 **Study materials and Methods**

350 **A description of study sites**

351 Mongolia's diverse geography and climatic conditions provide a unique backdrop for understanding  
352 particulate matter pollution and its impacts. This study focuses on four distinct locations across  
353 the country, selected to represent varying urban and desert environments with different elevations  
354 and climatic conditions.

355 Ulaanbaatar (47.92°N, 106.92°E): The capital city, situated at an elevation of 1350 m,  
356 characterized by high urban activity and associated air pollution.

357 Dalanzadgad (43.57°N, 104.42°E): A Gobi Desert town at an elevation of 1470 m, representing  
358 arid and sparsely populated areas.

359 Sainshand (44.87°N, 110.12°E): Located at an elevation of 947 m, featuring semi-arid conditions.

360 Zamyn Uud (43.72°N, 111.90°E): A border town at 967 m elevation, characterized by cross-border  
361 trade activities.

362 Table 1 summarizes the geographical coordinates, elevations, and relevant site characteristics,  
363 while Figure 1 provides a spatial representation of the locations. These sites capture a wide  
364 spectrum of environmental conditions, facilitating a comprehensive assessment of particulate  
365 matter pollution.

366 **Data**

367 **Data Collection**

368 Particulate matter with aerodynamic diameters less than 2.5 (PM2.5) and 10 micrometers (PM10)  
369 were measured at these sites using an instrument that measures light scattering by air-borne  
370 particulates. Meteorological parameters, including wind speed, wind direction and visibility were  
371 determined by automatic instruments and are detailed in previous articles (Jugder et al., 2011,

372 2012; Nishikawa, Sugimoto). The instruments for measuring particulate matters were placed 2  
373 m above the ground level (AGL) at Dalanzadgad, Sainshand and Zamyn-Uud (Table 2.1). Wind  
374 sensors and visibility (meteorological optical range-MOR) sensors with a maximum measurement  
375 range of 20 km were installed at a height of 3 m AGL at the three Gobi sites. At the Ulaanbaatar  
376 site, the wind sensor height and a visibility sensor was placed at 15 m AGL. Datasets were  
377 obtained from measurements at Dalanzadgad, Sainshand, and Zamyn-Uud from January 2009  
378 to May 2018, and at Ulaanbaatar from the end of April 2008 to May 2020.

379 To improve the data quality, we removed spikes exceeding above  $7 \text{ gm}^3$  considering the reported  
380 extreme values (XXXXX Jugder, XXXX Tsatsral), unrealistic PM2.5 values exceed PM10 (pm2.5  
381 > pm10 \*1.1) and detected signals that invariate with an extended period caused by electricity  
382 shortage and equipment malfunctions for all sites. Further, we handled data each stations  
383 separately to remove suspective data, carefully. For example, In Sainshand station, ... was ...  
384 Prior to data quality improvement, there were missing data with percentages ranged from 10.3%  
385 to 23.6%, attributed to equipment malfunctions or adverse weather conditions. Ulaanbaatar  
386 demonstrated the highest data completeness for both PM2.5 (88.6%) and PM10 (89.7%),  
387 whereas Dalanzadgad recorded the lowest (PM2.5: 76.4%; PM10: 81.5%)(Table 1). After data  
388 quality improvement, missing data percentages has increased by XXXXXX. [Due to electricity  
389 shortage and equipment malfunctions contributed to the bad data, and missing data....]

390 The data used in the study are based on hourly means derived from 1 and 10 min averages. For  
391 trend analysis, we added the data derived after data filling with the procedure, detailed in the next  
392 section.

393 Data filling Missing data handling with the statistical packages At last, we filled the missing data  
394 with 3-hour maxgaps with imputeTS package for univariate time series, and larger gaps using  
395 mtsdi R package (well-used for time-series data), and improved the missing data percents by...  
396 from ... to ... Additionally, meteorological parameters such as wind speed, direction, and visibility  
397 are integrated into the analysis to elucidate their impact on PM levels.

398 The MTSDI method (Junger, Santos, and Ponce de Leon (2003), Junger and Leon (2012)) uses  
399 the EM algorithm with the Autoregressive Integrated Moving Average (ARIMA) method, also known

400 as Box–Jenkins model (Box et al. (2015), Meyler, Kenny, and Quinn (1998)). The data provided by  
401 ARIMA (p, d, q) depend on the number of autoregressive terms (p), the number of differences (d),  
402 and the number of terms in the moving average (q) (Meyler, Kenny, and Quinn (1998)). Default  
403 configuration was used. The mtdsi method is widely used to impute missing data like in cosmic  
404 data Fernandes, Lucio, and Fernandez (2017). Similar multiple imputation methods have been  
405 applied for multivariate solar data Zhang et al. (2020), highly univariate seasonal data even with  
406 the large amount of missing data Chaudhry et al. (2019), missin data imputation and modeling  
407 for leaching processes He et al. (2017). Recently, Motesaddi Zarandi et al. (2022b) used the  
408 mtdsi method to imputing missing data air pollution in Tehran (We used the complete data of  
409 temperature (°C), relative humidity (RH) (%), wind speed (m/s), barometric pressure (BP) (mbar),  
410 PM10, PM2.5, NO2, CO, and CVD variables to impute SO2 and O3 with the mtdsi R package.).

411 Spatial Representation Figure 1 illustrates the geographical distribution of study sites and the  
412 locations of meteorological stations. The visual contrast between urban (e.g., Ulaanbaatar)  
413 and desert (e.g., Dalanzadgad) environments underscores the spatial variability in air quality  
414 measurements across Mongolia.

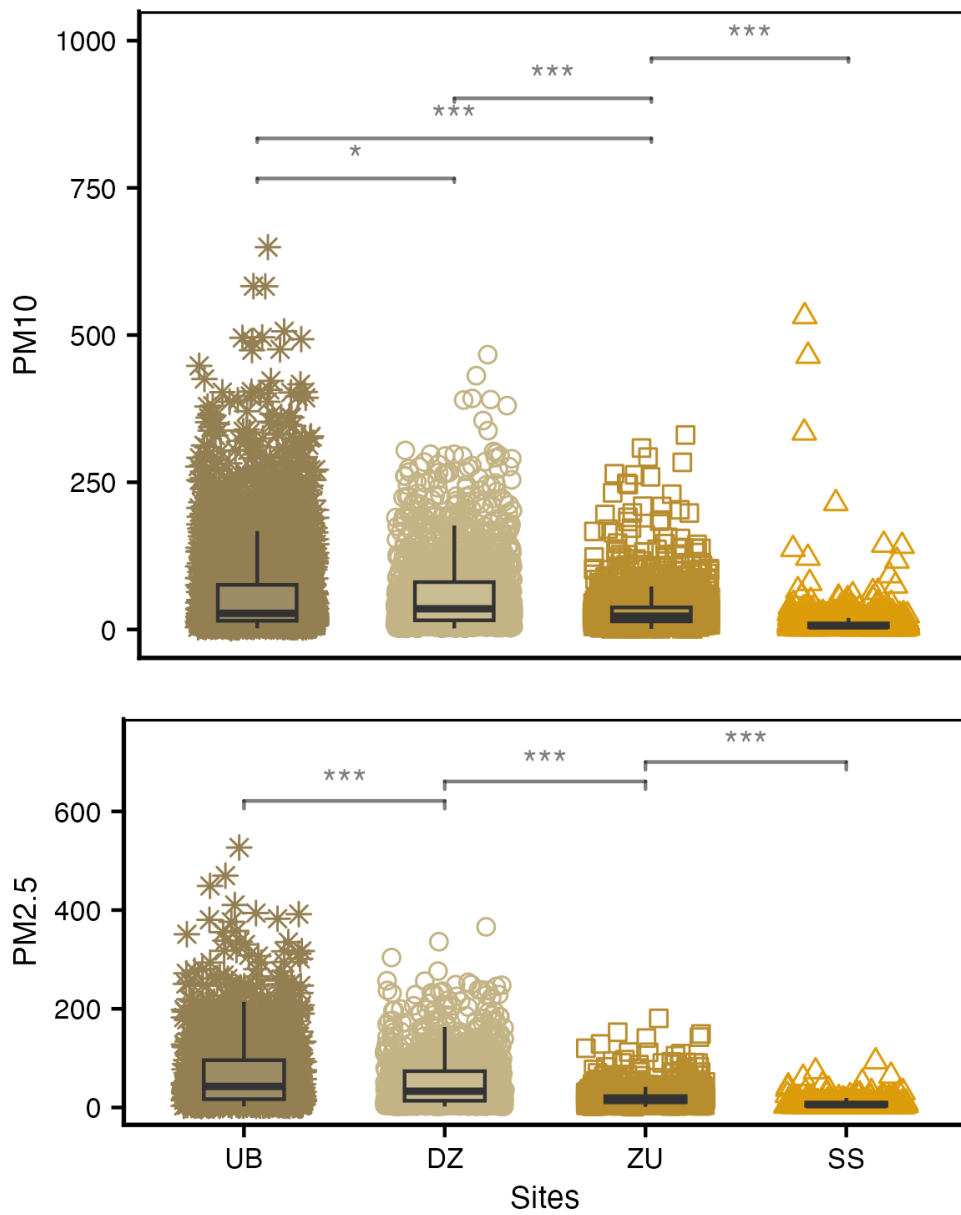


Figure 1: Distinct concentrations of coarse and fine particulates among sites

- 415 1. Compare the concentrations of PMs at UB is the 2. Significance level difference 3. Conclude

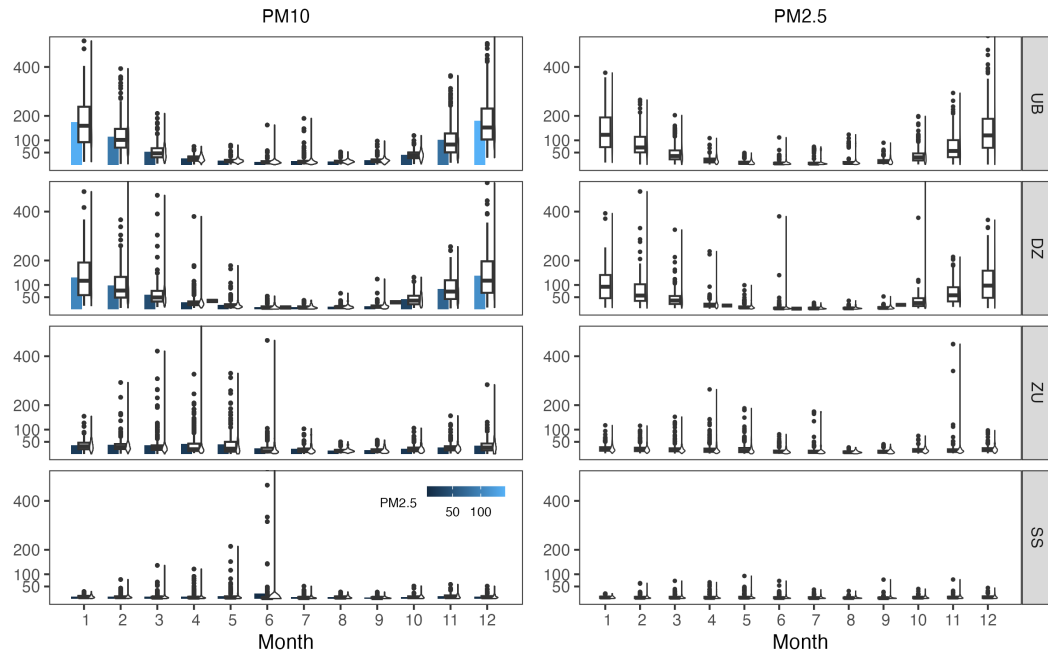


Figure 2: Annual variations of \$PM\_{10}\$ and \$PM\_{2.5}\$

- 416 1. Clear annual variations at UB and DZ from pm2.5 pollutions 2. at ZU, and SS has a  
 417 seasonally peaks episodic spring and late autumn from PM10

### Daily variations of PM<sub>10</sub> and PM<sub>2.5</sub> concentrations

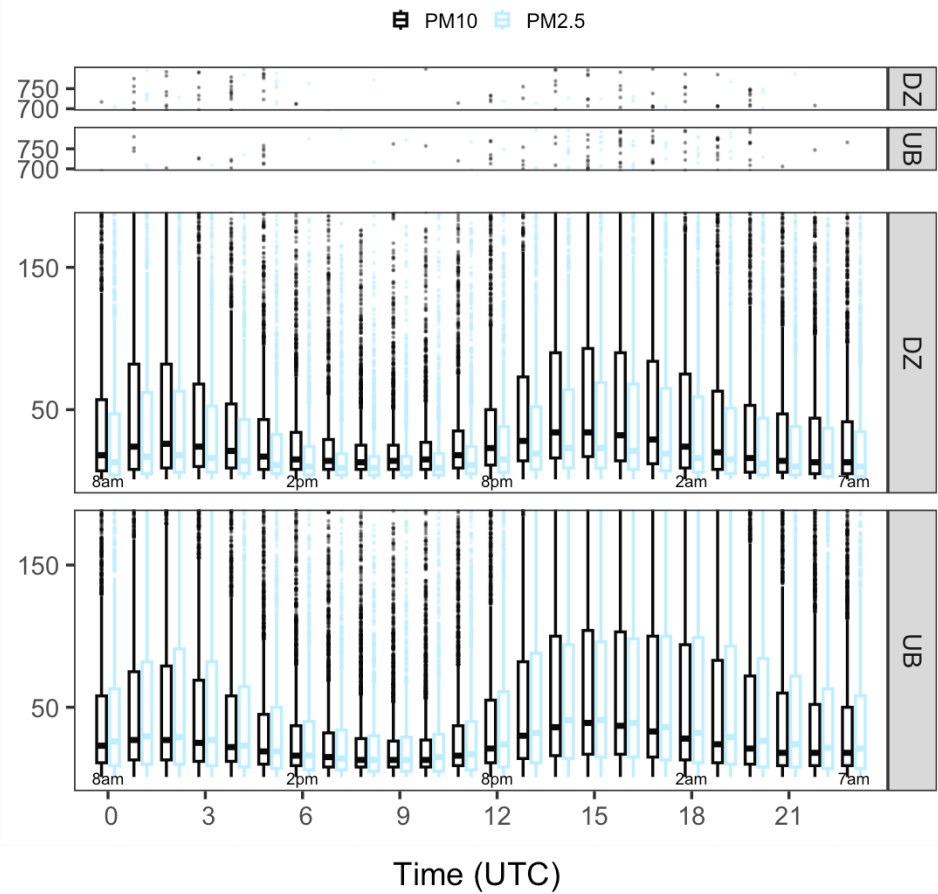


Figure 3: Daily variations of  $PM_{10}$  and  $PM_{2.5}$  at UB and DZ sites

418 **Meteorological influence on  $PM_{10}$  and  $PM_{2.5}$  variations**

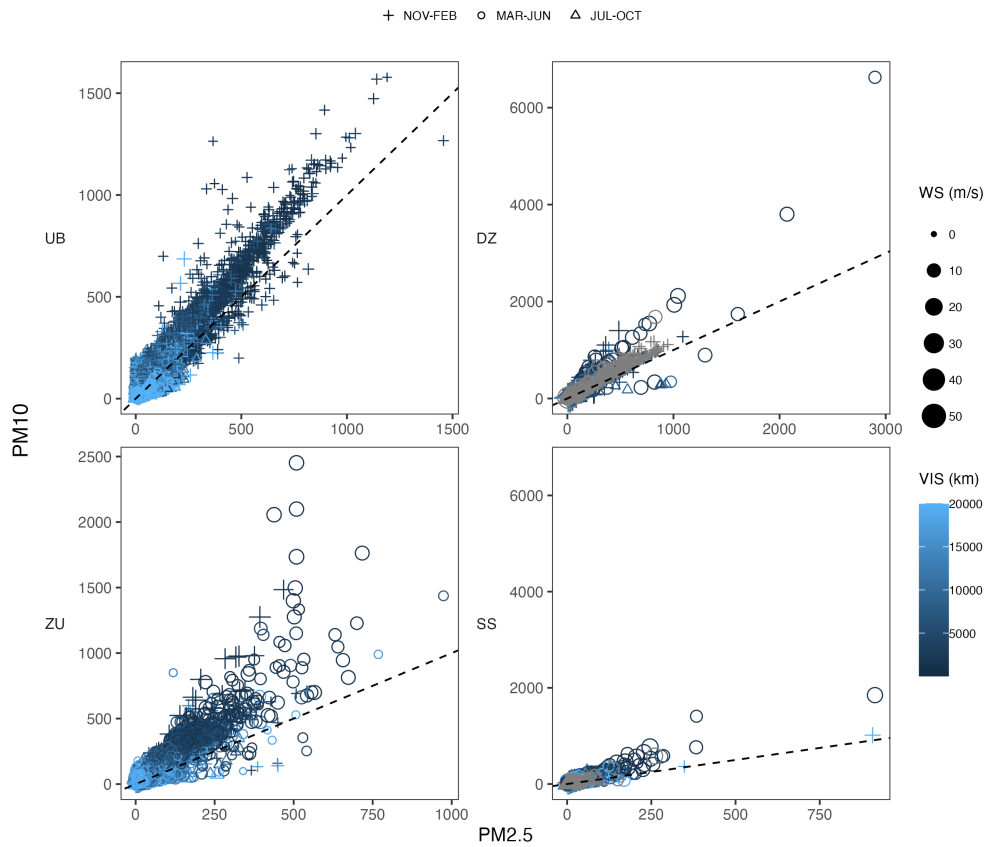


Figure 4: Relationships between meteorological major factors and variations of  $PM_{10}$  and  $PM_{2.5}$

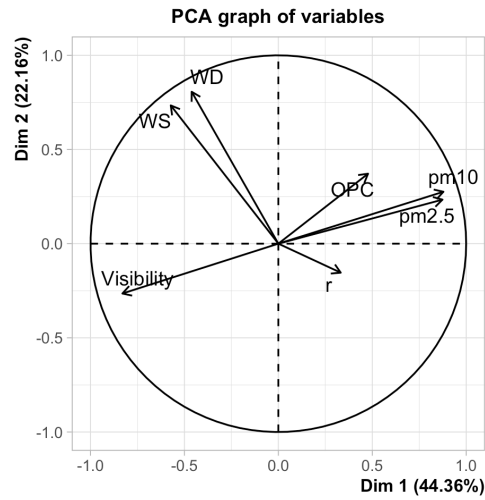


Figure 5: Spatio-temporal distinct feature of variations of  $PM_{10}$  and  $PM_{2.5}$  with PCA analysis

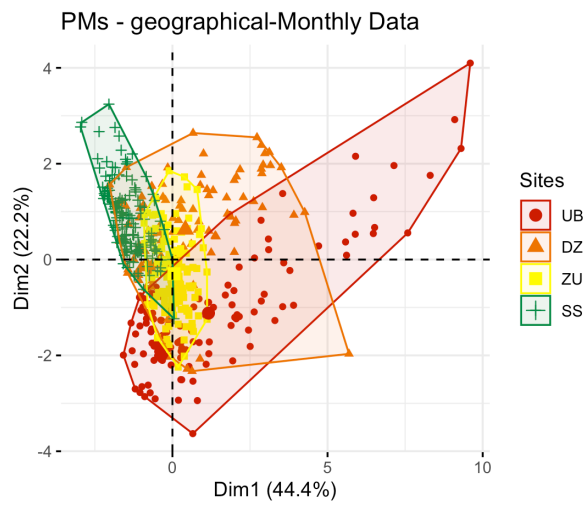
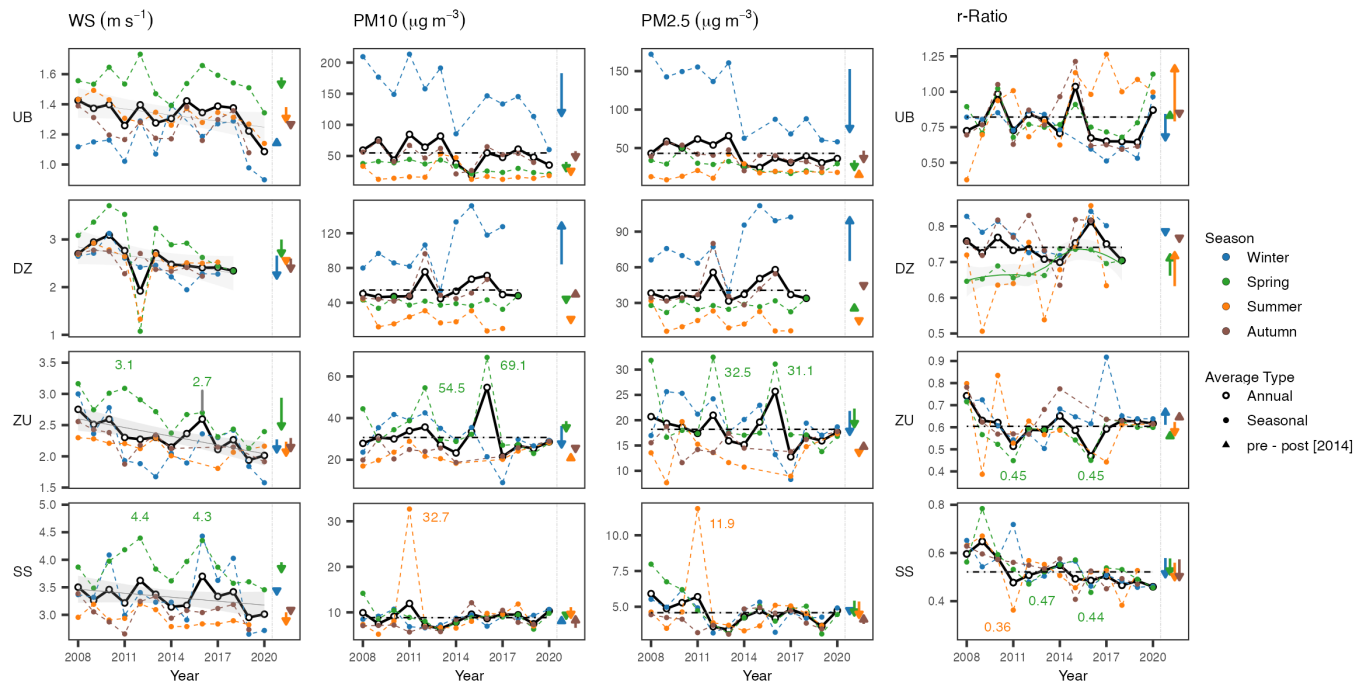
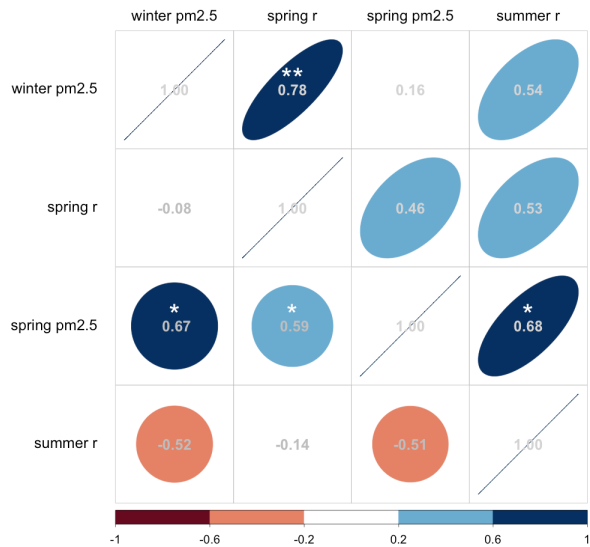


Figure 6: Patterns of meteorology and PMs at the 4 sites

419 Trends



420



421

<sup>422</sup> Now for some more text and then here is Table @ref(tab:lab2).

Table 1: This is table 2

Variables	Seasonal				Annual <b>N = 13<sup>1</sup></b>
	Winter N = 12 <sup>1</sup>	Spring N = 13 <sup>1</sup>	Summer N = 13 <sup>1</sup>	Autumn N = 12 <sup>1</sup>	
<b>UB</b>					
r	0.74 (0.15)	0.81 (0.14)	0.89 (0.24)	0.78 (0.20)	0.78 (0.13)
pm2.5	0.11 (0.04)	0.03 (0.01)	0.02 (0.01)	0.04 (0.01)	0.043 (0.014)
pm10	0.15 (0.05)	0.03 (0.01)	0.02 (0.01)	0.05 (0.02)	0.055 (0.019)
WS	1.15 (0.14)	1.54 (0.10)	1.33 (0.09)	1.25 (0.10)	1.33 (0.10)
WD	177 (29)	191 (11)	168 (6)	167 (12)	174.6 (7.4)
VIS	10,331 (2,932)	17,659 (1,579)	19,288 (903)	16,766 (1,727)	16,614 (1,753)
<b>DZ</b>					
r	0.78 (0.05)	0.69 (0.04)	0.67 (0.10)	0.77 (0.06)	0.741 (0.033)
pm2.5	0.080 (0.022)	0.027 (0.004)	0.014 (0.009)	0.042 (0.016)	0.041 (0.009)
pm10	0.10 (0.03)	0.04 (0.01)	0.02 (0.01)	0.05 (0.02)	0.055 (0.011)
WS	2.47 (0.33)	2.84 (0.73)	2.50 (0.44)	2.51 (0.22)	2.57 (0.32)
WD	239 (5)	232 (13)	223 (12)	230 (7)	230.97 (3.10)
VIS	12,146 (1,457)	15,469 (609)	17,080 (740)	15,169 (1,150)	15,001 (655)
<b>ZU</b>					
r	0.65 (0.10)	0.58 (0.07)	0.60 (0.14)	0.64 (0.08)	0.60 (0.07)
pm2.5	0.019 (0.005)	0.020 (0.007)	0.013 (0.004)	0.015 (0.002)	0.0182 (0.0032)
pm10	0.031 (0.009)	0.036 (0.013)	0.022 (0.004)	0.024 (0.004)	0.031 (0.008)
WS	2.16 (0.42)	2.66 (0.32)	2.15 (0.15)	2.21 (0.22)	2.32 (0.24)
WD	225 (17)	201 (9)	176 (10)	212 (7)	204.5 (6.1)
VIS	15,362 (1,534)	16,280 (1,218)	17,975 (832)	16,928 (844)	16,530 (877)
<b>SS</b>					
r	0.54 (0.08)	0.54 (0.09)	0.52 (0.09)	0.53 (0.06)	0.52 (0.06)
pm2.5	0.0046 (0.0009)	0.0049 (0.0014)	0.0048 (0.0023)	0.0041 (0.0006)	0.0046 (0.0008)
pm10	0.0086 (0.0014)	0.0090 (0.0020)	0.0100 (0.0074)	0.0079 (0.0019)	0.0088 (0.0015)
WS	3.38 (0.54)	3.86 (0.31)	2.94 (0.15)	3.05 (0.23)	3.32 (0.22)
WD	256 (10)	249 (10)	232 (6)	242 (6)	245.3 (3.7)

<sup>1</sup> N; Mean (SD)

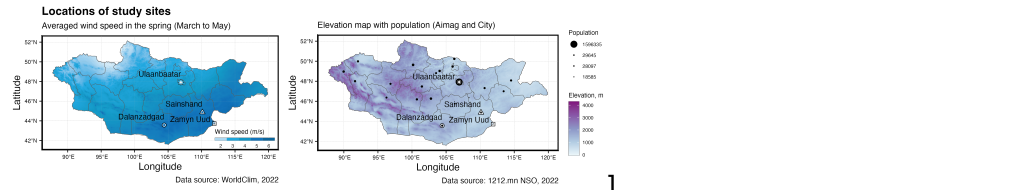
424 Now for some more text and then here is Table @ref(tab:lab3).

Table 2: This is table 3: Seasonal and Annual trends

Characteristic	Winter				Spring				Summer				Autumn			
	I N = 6 <sup>1</sup>	II N = 6 <sup>1</sup>	Difference <sup>2</sup>	P-value <sup>2</sup>	I N = 6 <sup>1</sup>	II N = 7 <sup>1</sup>	Difference <sup>2</sup>	P-value <sup>2</sup>	I N = 6 <sup>1</sup>	II N = 7 <sup>1</sup>	Difference <sup>2</sup>	P-value <sup>2</sup>	I N = 6 <sup>1</sup>	II N = 6 <sup>1</sup>	Difference <sup>2</sup>	P-value <sup>2</sup>
<b>UB</b>																
r	0.82 (0.05)	0.66 (0.17)	-0.16	0.067	0.80 (0.13)	0.82 (0.15)	0.01	0.9	0.75 (0.22)	1.01 (0.20)	0.26	<b>0.049</b>	0.80 (0.15)	0.77 (0.26)	-0.02	0.8
PM2.5 ( $\mu\text{g}/\text{m}^3$ )	0.15 (0.01)	0.07 (0.01)	-0.08	<b>&lt;0.001</b>	0.034 (0.008)	0.021 (0.005)	-0.01	<b>0.010</b>	0.018 (0.012)	0.020 (0.004)	0.00	0.7	0.047 (0.007)	0.032 (0.008)	-0.01	<b>0.008</b>
PM10 ( $\mu\text{g}/\text{m}^3$ )	0.18 (0.03)	0.11 (0.04)	-0.07	<b>0.004</b>	0.041 (0.003)	0.026 (0.005)	-0.02	<b>&lt;0.001</b>	0.024 (0.016)	0.020 (0.012)	0.00	0.6	0.058 (0.012)	0.043 (0.017)	-0.01	0.12
WS (m/s)	1.14 (0.09)	1.17 (0.19)	0.03	0.7	1.58 (0.09)	1.51 (0.11)	-0.07	0.3	1.38 (0.08)	1.28 (0.08)	-0.10	<b>0.050</b>	1.25 (0.09)	1.24 (0.12)	-0.01	0.8
WD (deg)	164 (11)	189 (37)	25	0.2	188 (12)	194 (9)	6.4	0.3	165.7 (6.8)	170.8 (3.3)	5.1	0.14	165 (12)	169 (12)	3.9	0.6
VIS (km)	7,769 (1,164)	12,893 (1,344)	5,123	<b>&lt;0.001</b>	16,174 (920)	18,931 (430)	2,757	<b>&lt;0.001</b>	18,801 (1,185)	19,706 (129)	906	0.12	15,393 (739)	18,140 (1,219)	2,747	<b>0.001</b>
<b>DZ</b>																
r	0.78 (0.04)	0.77 (0.06)	0.00	>0.9	0.662 (0.015)	0.722 (0.020)	0.06	<b>&lt;0.001</b>	0.63 (0.10)	0.73 (0.10)	0.10	0.2	0.77 (0.05)	0.76 (0.11)	-0.01	0.8
PM2.5 ( $\mu\text{g}/\text{m}^3$ )	0.065 (0.014)	0.102 (0.007)	0.04	<b>&lt;0.001</b>	0.026 (0.004)	0.029 (0.004)	0.00	0.4	0.016 (0.010)	0.012 (0.008)	0.00	0.5	0.042 (0.019)	0.042 (0.013)	0.00	>0.9
PM10 ( $\mu\text{g}/\text{m}^3$ )	0.084 (0.018)	0.132 (0.014)	0.05	<b>0.002</b>	0.040 (0.005)	0.040 (0.006)	0.00	>0.9	0.024 (0.012)	0.017 (0.010)	-0.01	0.3	0.054 (0.021)	0.054 (0.011)	0.00	>0.9
WS (m/s)	2.66 (0.25)	2.18 (0.16)	-0.48	<b>0.006</b>	3.00 (0.97)	2.64 (0.26)	-0.36	0.4	2.51 (0.59)	2.48 (0.06)	-0.03	>0.9	2.60 (0.21)	2.32 (0.09)	-0.28	<b>0.031</b>
WD (deg)	239.7 (4.6)	238.6 (6.1)	-1.2	0.8	233 (18)	232 (4)	-1.4	0.9	220 (14)	228 (7)	7.5	0.3	229.4 (7.8)	230.7 (4.3)	1.3	0.8
VIS (km)	11,175 (988)	13,603 (165)	2,428	<b>0.002</b>	15,448 (779)	15,495 (410)	47	>0.9	17,438 (691)	16,543 (454)	-895	<b>0.039</b>	15,023 (1,400)	15,459 (451)	436	0.5
<b>ZU</b>																
r	0.61 (0.09)	0.68 (0.10)	0.07	0.2	0.57 (0.09)	0.58 (0.06)	0.00	>0.9	0.62 (0.17)	0.56 (0.08)	-0.06	0.5	0.63 (0.09)	0.66 (0.07)	0.03	0.6
PM2.5 ( $\mu\text{g}/\text{m}^3$ )	0.022 (0.004)	0.017 (0.005)	0.00	0.077	0.022 (0.008)	0.019 (0.006)	0.00	0.4	0.014 (0.004)	0.013 (0.004)	0.00	0.8	0.0152 (0.0026)	0.0156 (0.0018)	0.00	0.8
PM10 ( $\mu\text{g}/\text{m}^3$ )	0.036 (0.007)	0.026 (0.009)	-0.01	<b>0.034</b>	0.039 (0.010)	0.034 (0.016)	0.00	0.5	0.022 (0.004)	0.023 (0.004)	0.00	0.8	0.024 (0.004)	0.024 (0.004)	0.00	0.9
WS (m/s)	2.27 (0.53)	2.06 (0.31)	-0.21	0.4	2.94 (0.18)	2.43 (0.20)	-0.51	<b>&lt;0.001</b>	2.23 (0.07)	2.01 (0.15)	-0.22	0.051	2.29 (0.24)	2.08 (0.11)	-0.21	0.10
WD (deg)	224 (12)	225 (21)	1.3	0.9	202 (11)	200 (7)	-2.7	0.6	180 (5)	171 (14)	-8.4	0.3	212.3 (8.9)	211.2 (3.5)	-1.1	0.8
VIS (km)	13,921 (834)	16,597 (523)	2,676	<b>&lt;0.001</b>	15,360 (988)	17,068 (763)	1,708	<b>0.007</b>	17,670 (797)	18,433 (744)	764	0.2	16,580 (919)	17,451 (353)	871	0.074
<b>SS</b>																
r	0.58 (0.09)	0.50 (0.05)	-0.08	0.092	0.58 (0.11)	0.51 (0.05)	-0.07	0.2	0.56 (0.11)	0.49 (0.06)	-0.07	0.2	0.57 (0.03)	0.49 (0.06)	-0.09	<b>0.014</b>
PM2.5 ( $\mu\text{g}/\text{m}^3$ )	0.0047 (0.0011)	0.0045 (0.0007)	0.00	0.6	0.0054 (0.0019)	0.0044 (0.0007)	0.00	0.2	0.0054 (0.0032)	0.0042 (0.0008)	0.00	0.4	0.0038 (0.0006)	0.0044 (0.0006)	0.00	0.11
PM10 ( $\mu\text{g}/\text{m}^3$ )	0.0082 (0.0016)	0.0090 (0.0011)	0.00	0.3	0.0094 (0.0028)	0.0086 (0.0012)	0.00	0.6	0.011 (0.011)	0.009 (0.002)	0.00	0.6	0.0066 (0.0007)	0.0091 (0.0018)	0.00	<b>0.017</b>
WS (m/s)	3.40 (0.37)	3.37 (0.68)	-0.03	>0.9	3.96 (0.31)	3.78 (0.31)	-0.18	0.3	3.05 (0.13)	2.83 (0.04)	-0.22	<b>0.008</b>	3.09 (0.29)	3.02 (0.16)	-0.07	0.6
WD (deg)	253 (8)	258 (12)	5.4	0.4	251 (5)	247 (13)	-4.3	0.4	232.9 (7.9)	230.1 (2.6)	-2.8	0.4	243.0 (5.6)	241.4 (6.9)	-1.6	0.7

<sup>1</sup> I and II denote pre and post [2014] with corresponding samplings of N, respectively; Mean (SD)

<sup>2</sup> Standardized Mean Difference; Welch Two Sample t-test



426

]

427 Now for some more text and then here is Table @ref(tab:lab1).

**Table 3:** This is table 1

**Table 1. Measured data**

SITE	COORDINATE	ELEVATION	Measured and collected data						Missing data	
			TOTAL <sup>1</sup>	WS&WD <sup>2</sup>	VIS <sup>3</sup>	OPC <sup>4</sup>	PM2.5 <sup>5</sup>	PM10 <sup>5</sup>	PM2.5	PM10
Ulaanbaatar	47.92°N, 106.92°E	1350 m	76656	72603	72886	33241	67940	68777	11.4%	10.3%
Dalanzadgad	43.57°N, 104.42°E	1470 m	60336	46332	33812	-	46066	49172	23.6%	18.5%
Sainshand	44.87°N, 110.12°E	947 m	59040	50513	49720	-	47111	47313	20.2%	19.9%
Zamyn Uud	43.72°N, 111.90°E	967 m	67392	62432	63948	-	57317	58512	14.9%	13.2%

<sup>1</sup> Equipment height: 15 meter at urban site (Ulaanbaatar), 2 meter at Gobi sites (Dalanzadgad, Sainshand and Zamyn Uud); <sup>2</sup> Measurement range: 0–60 m/s; 0–365 degrees. Instrument model: Wind speed and direction PGWS-100, Gill, England; <sup>3</sup> Range: 10–20 000 m. Visibility meter PWD10, Vaisala, Finland; <sup>4</sup> Optical Particle Counter; <sup>5</sup> Range: 0.003–100 mg/m<sup>3</sup>. Flow rate: 20 L/m, Suction rate: 2 L/m. Measured by Kosa monitor ES-640, TDK Co. LTD, Japan;

428

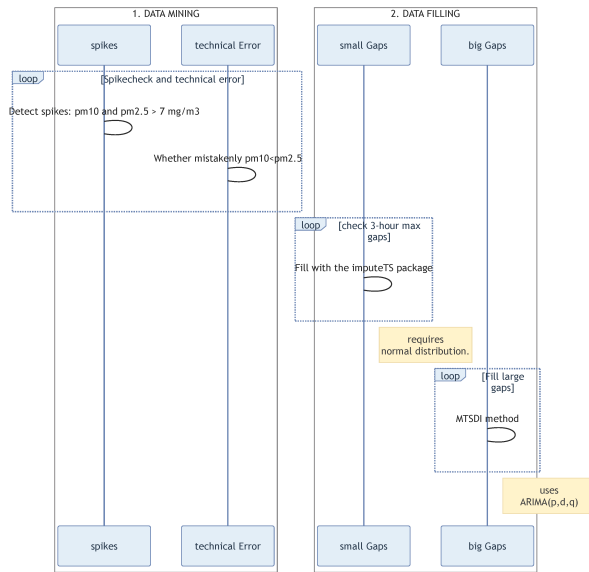


Figure 7: Scheme 1. Data handling procedure

429 **Supplements**

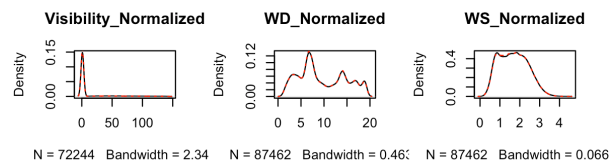
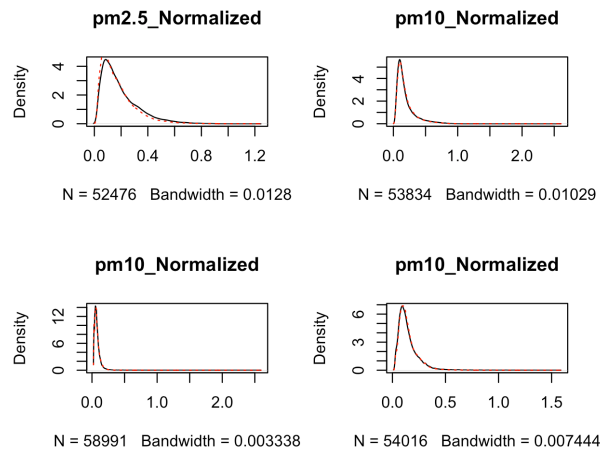


Figure 8: Figure 2. Data gap filling



430

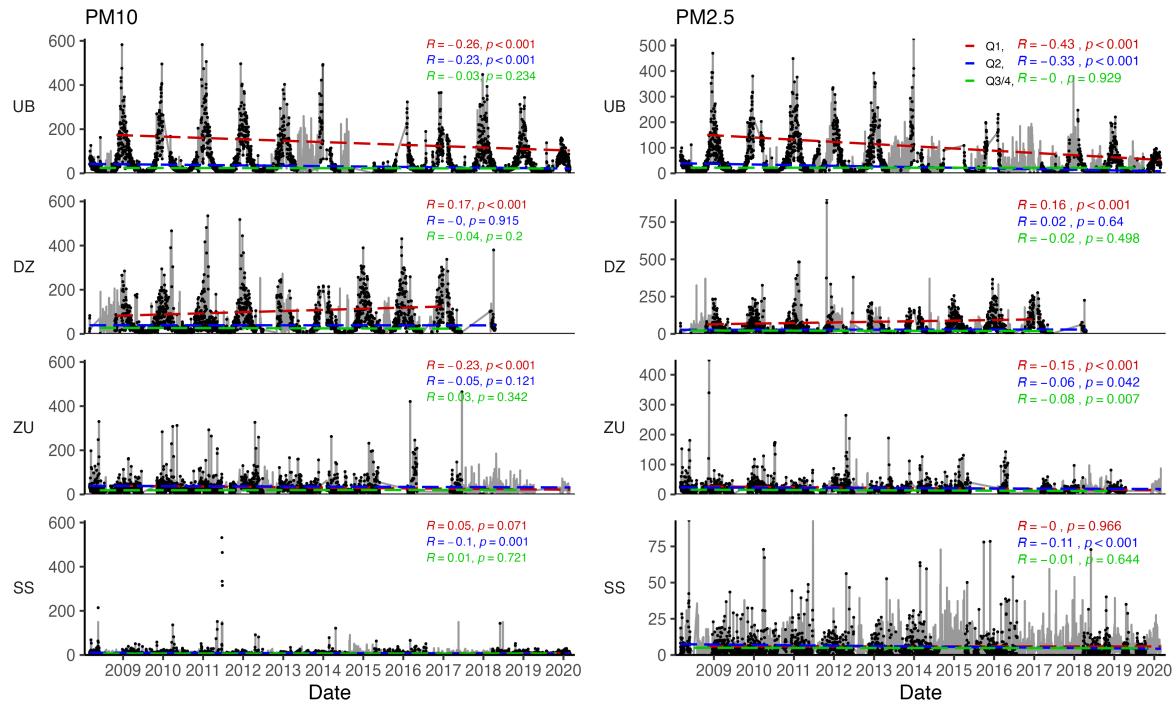


Figure 9: Interannual and seasonal trends of  $PM_{10}$  and  $PM_{2.5}$  variations

431 (1)

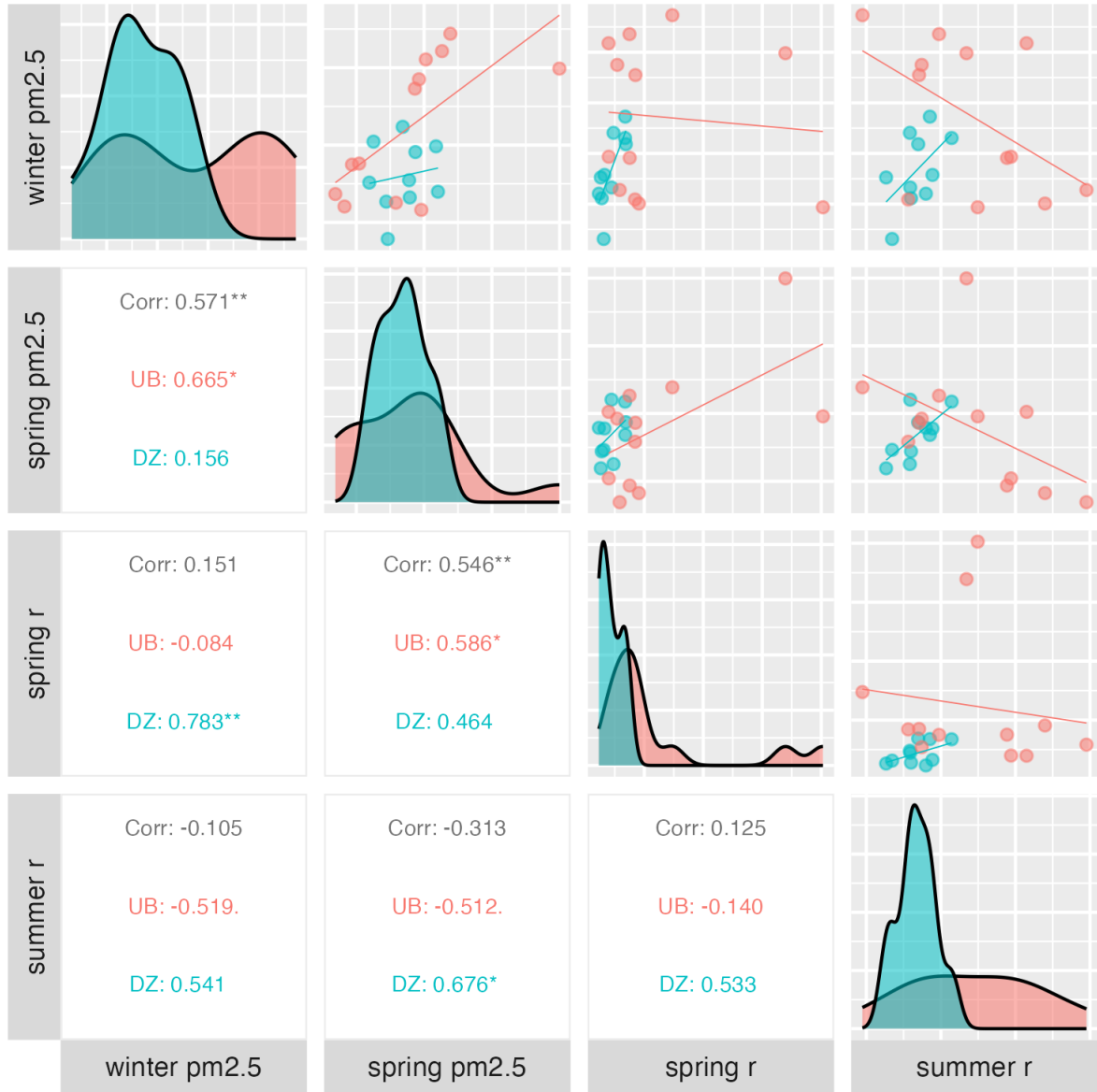


Figure 10: Interannual and seasonal trends of  $PM_{10}$  and  $PM_{2.5}$  variations

432 **References**

- 433 1. **Munkhtsetseg E, Shinoda M, Ishizuka M, Mikami M, Kimura R, Nikolich G.**  
2017. Anthropogenic dust emissions due to livestock trampling in a mongolian  
temperate grassland. *Atmospheric Chemistry and Physics* **17**:11389–11401.  
doi:10.5194/acp-17-11389-2017.